Int. J. Nanosci. Nanotechnol., Vol. 16, No. 2, June 2020, pp. 73-89

# Synthesis, Characterization, and Antibacterial Activity of ZnO Nanoparticles from Organic Extract of *Cola Nitida* and *Cola Acuminata* Leaf

**Asare Ebenezer Aquisman[1,2], Boon Siong Wee[1], Suk Fun Chin[1], Droepenu Eric Kwabena[1,2,*], Kyene Odoi Michael[4], Tomy Bakeh[1], Shafri Semawi[1] and Dapaah Samuel Sylverster[3]**

[1]Resource Chemistry Program, Faculty of Resource Science and Technology, Universiti Malaysia Sarawak 94300, Kota Samarahan, Sarawak, Malaysia.
[2]Graduate School of Nuclear and Allied Sciences, University of Ghana, AE1, Kwabenya-Accra, Ghana.
[3]St. Joseph's College of Education, Bechem, Brong Ahafo Region, Ghana.
[4]Department of Pharmaceutics, Centre for Plant Medicine Research, Mampong-Akuapem, Ghana.

(*) Corresponding author: kobladodzie01@yahoo.com
*(Received: 07 November 2019 and Accepted: 31 December 2019)*

***Abstract***

*The study aimed at the synthesis and antibacterial activity of ZnO nanoparticles (NPs) from organic extracts of Cola nitida and Cola acuminata leaf using zinc chloride ($ZnCl_2$) and zinc acetate dihydrate [$Zn(CH_3COO)_2{\cdot}2H_2O$] as precursors on selected Gram positive and Gram negative microbes: Staphylococcus aureus, Exiguobacterium aquaticum, (Gram +ve) and Escherichia coli, Klebsielia pneumonia, Acinetobacter baumanni (Gram –ve). Spherical and flake-like nanostructures were recorded by Scanning Electron Microscopy (SEM) for C. acuminata and C. nitida respectively for the two precursors used. The average particle size and crystallite size determined by Transmission Electron Microscopy (TEM) and X-ray Diffraction (XRD) for C. acuminata and C. nitida were in the range of 32.15-43.26 nm; 69.12-84.26 nm and 14.69-17.12 nm; 23.68-23.96 nm respectively. Energy-dispersive X-ray spectroscopy (EDX), UV- visible spectroscopy (UV-vis), Atomic Absorption Spectroscopy (AAS) and Fourier-transform infrared spectroscopy (FT-IR) techniques were used to observe the purity and surface functional groups of the samples. Spectra peaks at 440-458 $cm^{-1}$ and 364-370 nm confirmed the presence of ZnO in the samples by FT-IR and UV-vis, whereas AAS at 213.9 nm wavelength further confirmed elemental zinc with a percentage atomic weight of 71.37% as against 69.50%, 18.8% and 11.1% for Zinc, Oxygen and Carbon by EDX. Data from the antibacterial activity studies show an increase in inhibition rate as concentration of the ZnO NPs increases in concentration from 25-1000 ppm. ZnO NPs from the two extracts recorded the highest inhibition rate in Acinetobacter baumanni of approximately 88% and 49% using $ZnCl_2$ and $Zn(CH_3COO)_2{\cdot}2H_2O$ respectively.*

***Keywords:*** *Precursor, Functional groups, Microscopy, Nanostructure, Spectroscopy*.

## 1. INRODUCTION

In recent years, microbial infection has become the cause of morbidity and mortality [1-3] and as a result, their causative agents (virus, bacteria, pathogenic fungi, protozoa) have developed resistant strains that withstand their clinical treatment using concomitant anti-drugs [4]. When the highly potent antibiotics are used, they generate various side effects, thus they are reserved only for critical infectious diseases. Currently, new methods for combating antibacterial drug resistance are being researched [5] resulting in the biosynthesis of nanoparticle with their diverse properties like chemical stability, catalytic activity,

electrical conductivity, anti-inflammatory activities and antimicrobial [6-8]. These properties are regulated by critical characteristics exhibited by nanoparticles and they include their size, shape distribution, lower toxicity and high surface-to-volume ratio [9-10]. Nano-particles have different applications in catalysts, sensors, electronic components, diagnostic imaging, pharmaceutical prod-ucts, drug delivery, cancer therapy, cosmetic industry and biosensors [7, 11-12].

Zinc oxide nanoparticles (ZnO NPs) can be synthesized through different technique-es including microwave-assisted synthesis, sol–gel, spray pyrolysis, chemical vapour deposition, co-precipitation, thermal decomposition, hyd-rothermal and com-bustion methods, wet chemical route, vapour phase process, precipitation and sonochemical method [13-21]. These chemical methods of synthesis are not environmentally friendly due to their chemical toxicity to the environment and high energy demand. Because of these draw backs, green synthesis or biosynthesis using environ-mentally friendly microorganisms (plant genus, biodegradable polymers (chitosan), bac-teria and fungi) has been accepted as a promising technique to remedy the constraints accompanied with the above-mentioned methods [22-23]. Biosynthesis often involves the use of plant extracts in single steps, clean, safe and cost effective approach [24]. Of late, plant extracts are employed and utilized due to their availability, biocompatibility, stability, as well as their ability to serve as capping agents for stabilization of the NPs [25-27]. CuI nanostructures using watermelon, cherry and carrot juices were synthesized for the first time for the removal of organic dyes [27]. Numerous studies were also being conducted into the treatment of various biomolecules using biosynthesized nanoparticles from different plants extra-cts. Notable among the plants used are Vaccinium arctostaphylos, Passiflora caerulea, Amaranthus Tricolor, Albizia lebbeck, Callistemon citrinus, and Carica papaya [28-33].

Biosynthesized ZnO NPs used for antibacterial purposes have several modes of action. First, they disrupt the integrity and potential membrane of the bacteria. Secondly, the ZnO NPs form reactive oxygen species (ROS) and induce nitrogen reactive species to inhibit several specific enzymes and finally cause the death of the cell. ZnO NPs could also generate hydro-gen peroxide; penetrate and cause injury to the cell membrane and subseq-uently prevent the development of the cells [34]. This is as a result of the affinity between ZnO and bacterial cells [35]. ZnO NPs are considered ideal potential antibacterial reagent to replace some antibiotics due to selective toxicity [36-37] as well as their effective inhibition of some bacteria such as dehydrogenase [38].

Cola nut is a traditional plant which is often eaten as snacks especially among the elderly in West Africa; Nigeria and Ghana. Cola nut belongs to the plant family Sterculiaceae, with about 125 species of trees native to the tropical rainforests of Africa. Of these, two species are particularly very common among the Yorubas of South Western Nigeria and Ghana; these are *Cola nitida* and *Cola acuminata*. Cola nut is chewed in many West African cultures, either individually or in group settings and is often used ceremonially [39]. It contains a large amount of caffeine and theobromine and is used as a stimulant [39,40]. Some benefits of Cola include enhancement of alertness and physical energy, elevation of mood, increase in tactile sensitivity, suppression of appetite and hunger and also used as an aphrodisiac [39,41]. The caffeine in the nuts also acts as a bronchodilator, hence, used to treat whooping cough and asthma [39,42]. Approximately 20% of known Cola nut plants have been used in pharmaceutical studies, impacting the healthcare system in positive ways such as treating cancer and harmful diseases [43].

In West Africa, the search for the benefits of cola nut against microbes has been grossly over looked. It is therefore imperative to fully explore, the biological activities for which cola nuts are needed. Hence, the study aimed at the synthesis, characterization, and antibacterial activity of ZnO nanoparticles from organic extract of *C. nitida* and *C. acuminata* Leaf.

## 2. METHODS AND MATERIALS

### 2.1 Plant Collection

Leaves of C. *nitida* and C. *acumunata* were collected from the Kakum national park in the central region of Ghana, West Africa in July 2018. The fresh green leaves of the two plant species were dried under room conditions for two weeks and grounded into powder form before been processed for extraction.

### 2.2 Preparation of Plant Extracts

Solvent extraction method was used as a technique to get the extracts from the leaves of *C. nitida* and *C. acuminata* as reported by [44]. A weighed mass of 1000.00 g each of the grounded leaves samples of both plants were soaked in methanol in a ratio of 1:3 at room temperature for 48 hours. The mixture was filtered to obtain the filtrate using a filter paper and the residue was re-extracted with fresh methanol for another 48 hours and filtered. All the filtrates (extracts) were composited and rotary evaporated using Heidolph Laborota 4000 to obtain a concentrate of hexane crude extract.

### 2.3 Synthesis of ZnO Nanoparticles

ZnO NPs were prepared as reported by [33] but with some modifications. A weighed mass of 9.15 ± 0.1 g (0.05 mol) of $Zn(CH_3COO)_2{\cdot}2H_2O$ and 2.80 ± 0.1 g of KOH were each dissolved in 50 ml of absolute ethanol ((HmBG Chemicals) in a 250 ml Schott bottle and heated under 60 ± 2 °C with constant stirring using Electric Stirring Hotplate (FAVORIT). After total dissolution of the two solutions, the KOH solution was drained dropwise from a burette into the $Zn(CH_3COO)_2{\cdot}2H_2O$ solution slowly at 60 ± 2 °C temperature with vigorous stirring in order to adjust the pH of the solution to 12. The stirring was done for an hour until white precipitate of zinc oxide was formed. A measured volume of 50 ml each of the organic plant (leaf) extracts of *C. nitida* and *C. acuminata* from a burette were allow to drain drop wise into each mixture separately under constant stirring at 20 ± 2 $^oC$ temperature with a magnetic stirrer for 3 hours. The solutions were allowed to cool at room temperature where the precipitate was separated from the supernatant by centrifuging at 4000 rpm for 30 minutes using Fleta 5, Hanil. The solid zinc oxide precipitate was thoroughly washed and dried under hot air in an oven at a temperature of 80 $^oC$ for four hours, cooled in a desiccator before been preserved in air-tight container for characterization.

### 2.4 Characterization and Instrumental Analysis of ZnO Nanoparticles

Different characterization techniques were employed to determine the existence and purity of the synthesized ZnO NPs.

*UV–Vis Spectra Analysis*

The optical property of the synthesized ZnO NP sample was determined by measuring its maximum absorbance using UV–Vis spectrophotometry (UV-1800 SHIMADZU). The NPs was dispersed in 95 % Absolute ethanol and sonicated for 10 minutes before the absorbance analysed in the range of 300–400 nm.

*Scanning Electron Microscopy (SEM) Analysis*

The morphology of ZnO NPs was determined using scanning electron microscopy (SU3500, Hitachi) with spectral imaging system Thermo Scientific NSS (EDS) and detector tape (BSE-3D) with acceleration voltage of 10.0 kV, working distance of 11.6 mm and a pressure of 40 Pa. Before the SEM

imaging, the dry powdered solid ZnO NPs were coated on an aluminium plate with the help of adhesive membrane on the aluminium plate.

*Transmission Electron Microscope (TEM) Analysis*

The morphological features especially the size and shape of ZnO NPs was determined using TEM (JEOL JEM-1230, Japan). Dry powdered ZnO NPs were first diluted with absolute ethanol (95%) and sonicated with ultrasonic cleaner (Elma, Germany) for 10 minutes. A volume of 4 µl of the solution sample was loaded onto a Foamvar film Copper grid (FF300-Cu) before being observed under TEM.

*X-ray Diffraction (XRD) Analysis*

The biosynthesized samples from the two precursors of the two plant species were characterized using X-ray Diffraction, XRD, (Xpert Pro MPD PW3040/60) for their crystal structure and crystallite size. Diffraction patterns from the XRD analysis in Figure 1 (A-D) were obtained using X-ray diffractometer with Cu-Kα radiation of 40 kV and 30 mA with step size of 0.017°.

*Fourier Transform Infra-Red Spectroscopy (FT-IR) Analysis*

Surface functional groups present in the synthesized ZnO NPs was analysed using FT-IR (Thermo scientific Nicolet iS10, US) with spectral range of 4000–400 $cm^{-1}$ at a resolution of 4 $cm^{-1}$. The characterization involved mixing the dry powdered ZnO NPs with Potassium bromide (KBr) in a ratio of 1: 19 [45]. The sample was then placed in the metal hole, pressed until the sample was compressed inside the hole which was used for the analysis.

*Energy-dispersive X-ray Spectroscopy (EDX) Analysis*

The purity of the ZnO NPs was determined with EDX (JEOL 6390LA, Japan). The ZnO NPs were diluted with absolute ethanol (95%) and sonicated with ultrasonic cleaner (Elma, Germany) for 10 minutes. Then, 4 µl of the liquid sample was loaded onto an aluminium plate before being analysed with the EDX.

*Atomic Absorption Spectroscopy (AAS) Analysis*

Confirmation of the presence of Zinc in the synthesized samples was carried out using AAS. A known concentration of the sample was prepared and analysed for the presence of the elemental Zinc using AAS (iCE 3000 Series AA, Thermo Scientific). Air-acetylene was used as fuel at approximately 2300 ℃ and flowed at 0.9 L/min. Doubled-beam optics with monochromator reduced the detection limits and provided higher accuracy. The various parameters used in the analysis are illustrated in Table 1.

***Table 1.*** *AAS parameters used in the analysis of the synthesized ZnO samples*

| Parameter | Characteristics |
|---|---|
| Wavelength (nm) | 213.9 |
| Flame type | Air-$C_2H_2$ |
| Nebulizer uptake (s) | 4 |
| Burner height (mm) | 14.2 |
| Lamp current (%) | 75 |
| Rescale limit (%) | 10 |
| Standards (mg/L) | 0.3000, 0.6000 and 1.000 |
| Acceptable fit | 0.995 |
| Detection limit (mg/L) | 0.0033 |

**2.5 Preparation of Test Samples**

The synthesized ZnO nanoparticle was tested using disc diffusion method on nutrient agar medium [46]. The preparation of test samples follows the procedure reported by, [33] where 1000 µg/mL stock sample from the synthesized ZnO sample was prepared and from which serial diluted concentrations of 10, 50, 100, 250, 500, and 1000 ppm were obtained for the study.

**2.6 Preparation of Bacteria Broth**

The bacteria used for the activity of the biosynthesized ZnO NPs were obtained from the stock culture provided by

Virology Laboratory, UNIMAS (Universiti Malaysia Sarawak). The procedure for bacteria broth preparation follows the one reported by, [33] where a weighed mass of 2.60 g of the dried broth was dissolved (in 200 mL deionized water) and autoclave at a temperature of 121 °C. The bacterial was incubated with a shaker at a temperature of 37 °C [44] for 16 h. The optical density (OD) of the bacterial broth after incubation was computed by UV Mini Spectrophotometer (1240 SHIMADZU) at wavelength 575 nm and compared to the standard (0.6-0.9).

### 2.7 Plate Inoculation

Inoculation of the bacteria for this study follows the procedure reported by, [33] where 1 mL of the prepared broth was streaked over the entire agar plate surface in four different directions using sterile cotton bud. A 10 µL volume of the organic test extract of concentrations 10, 50, 100, 250, 500 and 1000 µg/mL were each pupated onto the prepared discs (6 mm diameter) and gently pressed onto the agar plate and left for 10 min at room temperature. A pupated disc with methanol and 30 µg of tetracycline were used as negative and positive controls respectively. Each of the test samples were tested in triplicate for the bacterium used. The plate samples were then incubated at a temperature of 37 °C for 24 h before the inhibition zone around every sample disc being examined. The inhibition zone was computed in diameter (mm) to show the presence of antibacterial activity for all the samples compared to the positive control.

### 2.8 Statistical Analysis

The inhibition zone diameter data were computed using one-way analysis of variance (ANOVA) with differences considered at $P$ value < 0.05.

## 3. RESULTS AND DISCUSSIONS

*Morphological Analysis*

*SEM*

The micrographs of ZnO nanostructures from extracts of *C. acuminata* using $ZnCl_2$ and $Zn(CH_3COO)_2{\cdot}2H_2O$ as precursor showed high aggregation of NPs with spherical shape (Fig 1B & 1D) as similar to structures documented by [47], whereas ZnO nanostructures from *C. nitida* extracts from both precursors produced well dispersed flake-like morphology (Fig 1C) and flake-like-shaped structures aggregated to form flower-like structures (Fig 1A).

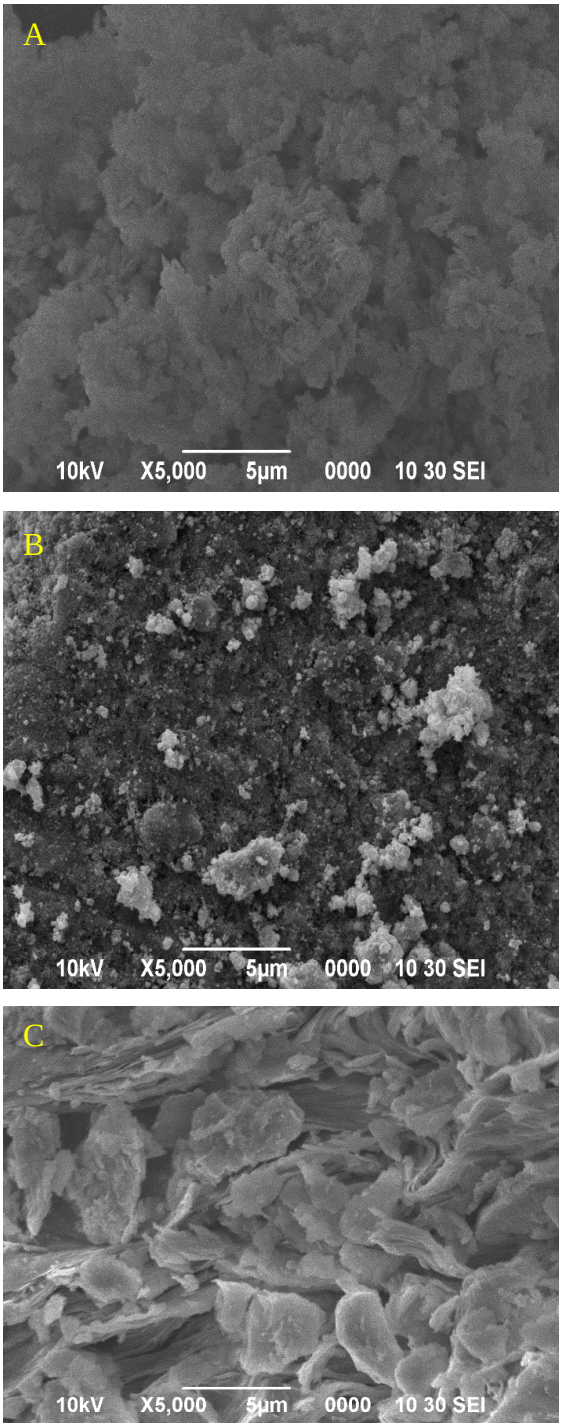

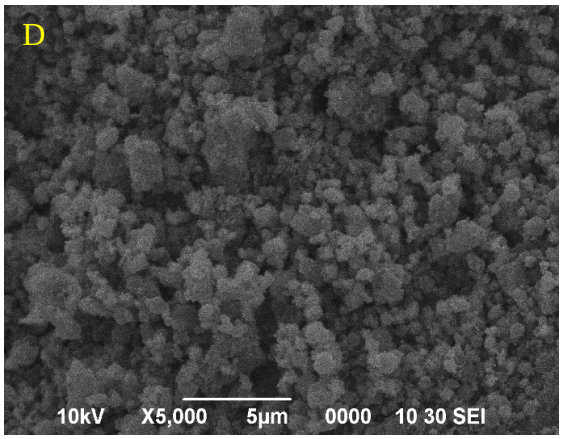


***Figure 1.*** *SEM micrographs of ZnO nanostructures synthesized with $ZnCl_2$ from methanol extract of (A) C. nitida (B) C. acuminate, and SEM micrographs of ZnO nanostructures synthesized with $Zn(CH_3COO)_2{\cdot}2H_2O$ from methanol extract of (C) C. nitida (D) C. acuminata*

The results for the SEM analysis showed that the plant part used in the extract affected the shape of the nanoparticles produced. This aggregation might be due to polarity and electrostatic attraction of ZnO nanoparticles as documented by [48]. Similarly, nearly spherical shaped structures were produced when *Vaccinium arctostaphylos* L. fruit extract was used in synthesizing ZnO NPs using zinc nitrate as precursor as documented by [28].

In another study by [49], investigations into the effect on morphology of ZnO NPs was carried out on two precursors; Zinc acetate and Zinc nitrate using *L. nobilis* leaves aqueous extract as a precursor. Growth of ZnO molecules were slow, where spherical structures were formed and eventually aggregated into small bullets with particle size in the range of 21-25 nm in the case of zinc acetate. On the other hand, spherical ZnO NPs were formed which finally aggregated to form flower-shaped bundles with particle size of 47 nm when zinc nitrate was used as a precursor.

*TEM Analysis*

TEM image of ZnO NPs was observed to ascertain the morphology and size of the synthesized material (Figure 2). Nanostructures of ZnO from *C. acuminata* extracts with $ZnCl_2$ and $Zn(CH_3COO)_2{\cdot}2H_2O$ as precursor (Fig. 2B & 2D) revealed spherical shapes as reported in the SEM micrographs with average particle size of 43.26 nm and 32.15 nm respectively.

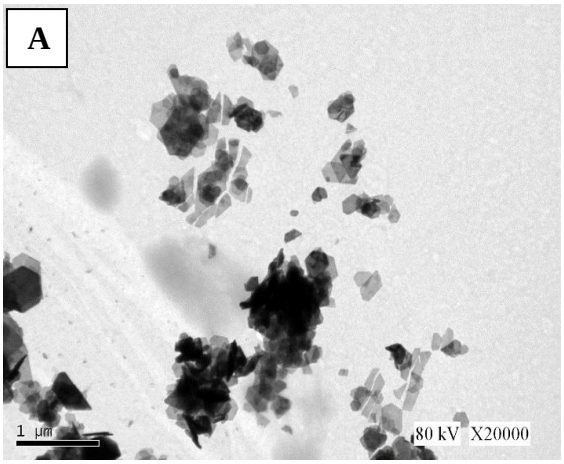


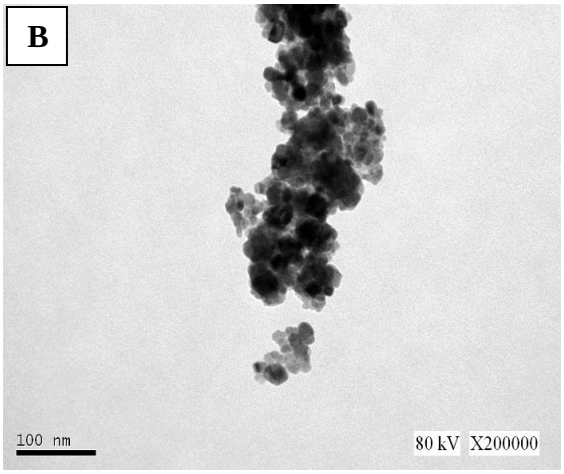


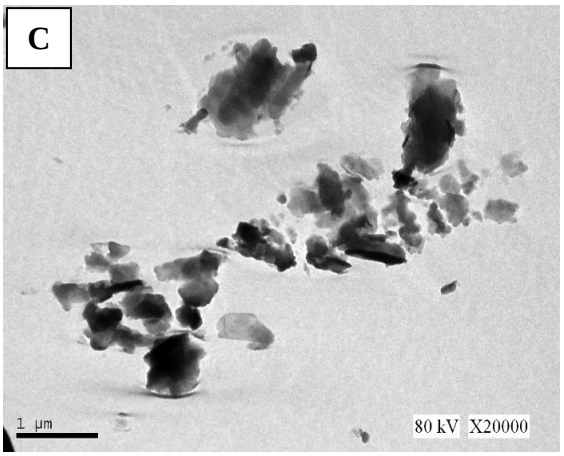

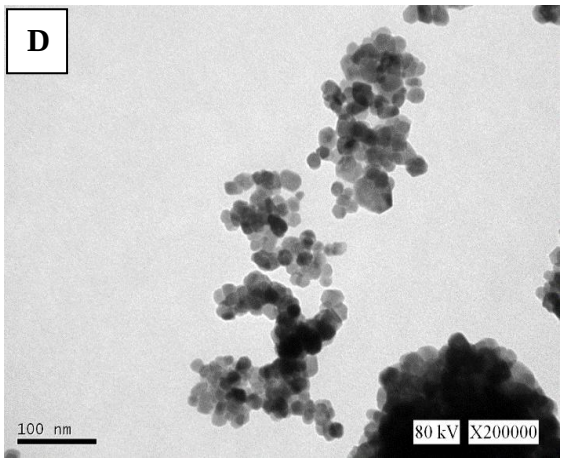


***Figure 2.*** *TEM images of ZnO nanostructures synthesized with $ZnCl_2$ from methanol extract of (A) C. nitida (B) C. acuminate, and TEM images of ZnO nanostructures synthesized with $Zn(CH_3COO)_2{\cdot}2H_2O$ from methanol extract of (C) C. nitida (D) C. acuminata*

The TEM result conforms to the result obtained by similar studies by [50]. On the other hand, ZnO NPs synthesized from *C. nitida* using the two precursors gave irregularly shaped structures of polyhedron (Fig 2A & 2C) as similar to results by [51], when *Corymbia citriodora* leaf extract was used in the synthesis of ZnO. The average particle size realised in this study for the above samples were 69.12 nm and 84.26 nm for $ZnCl_2$ and $Zn(CH_3COO)_2{\cdot}2H_2O$ respectively which was in line with reported particle sizes determined by [52-53].

*XRD results*

X-ray diffraction was further conducted to confirm the ZnO phase of the nanoparticles. The patterns are shown in Figure 3 where the FWHM value for every peak assigned for particle size calculation are also shown in Table 2. The crystallite size of the nanostructures was obtained using Debye-Scherrer's formula;

$$D = \frac{K\lambda}{(\beta cos\theta)} \quad (1)$$

$$\beta = \sqrt{\beta_{FWHM}^2 - \beta_0^2} \quad (2)$$

where; D – crystallite size, $\lambda$ – wavelength of radiation, K - shape factor = 0.89, β - the peak broadening after removing the instrumental broadening, $\beta_{(FWHM)}$ is the full width half maximum of the diffraction peak and $\beta_0$ is the correction factor for instrumental broadening ($0.07^o2\theta$). All detectable peaks can be indexed to ZnO wurtzite structure with ICSD Number (ICSD: 98-000-9346) and PDF Number (Experimental and calculated powder diffraction data) of 36-1451 and 01-074-0534 respectively.

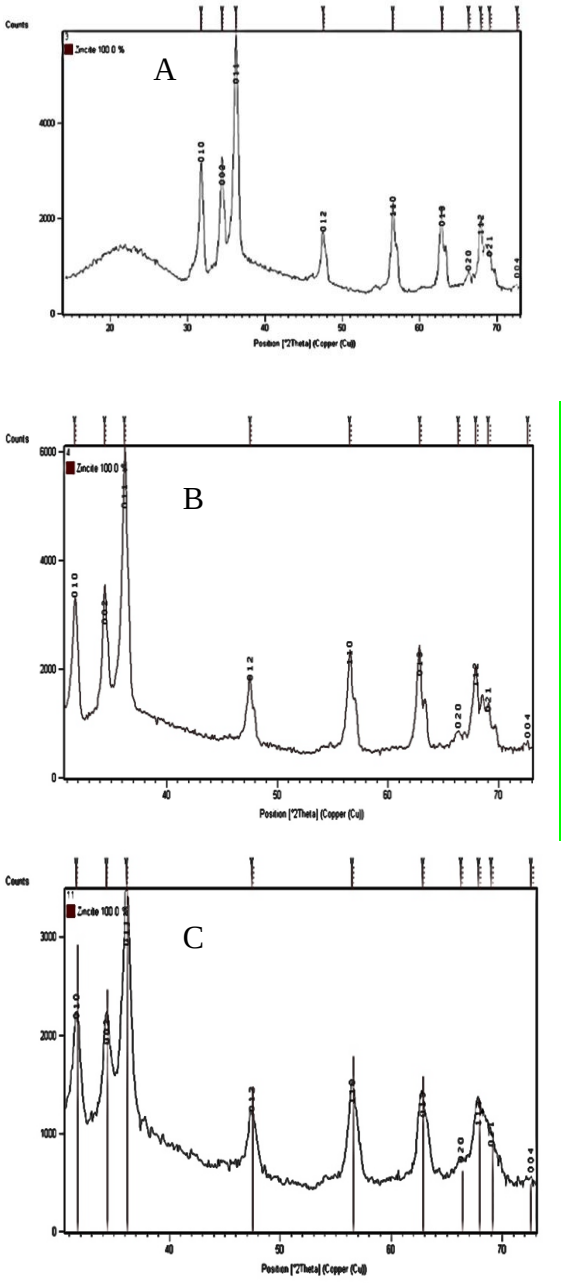

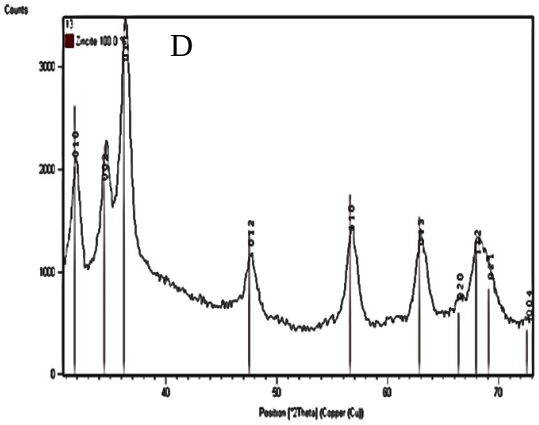


***Figure 3.*** *XRD patterns of ZnO nanostructures synthesized with $ZnCl_2$ from methanol extract of (A) C. nitida (B) C. acuminate, and XRD patterns of ZnO nanostructures synthesized with $Zn(CH_3COO)_2{\cdot}2H_2O$ from methanol extract of (C) C. nitida (D) C. acuminate*

***Table 2.*** *Average crystallite size calculation for C. acuminata extracts with $ZnCl_2$ (A) and $Zn(CH_3COO)_2{\cdot}2H_2O$ (B) as precursors.*

A

| 2θ | hkl | FWHM (β) | D (nm) |
|---|---|---|---|
| 31.6 | 010 | 0.2922 | 25.86083 |
| 34.3 | 002 | 0.4546 | 16.50704 |
| 36.1 | 011 | 0.5196 | 14.36904 |
| 47.3 | 012 | 0.3247 | 22.15504 |
| 56.5 | 110 | 0.3897 | 17.74725 |
| 62.7 | 013 | 0.5196 | 12.90353 |
| 67.7 | 113 | 0.6336 | 10.2918 |
| **AVERAGE CRYSTALLITE SIZE = 17.12** | | | |

| | | | |
|---|---|---|---|
| 47.5 | 012 | 0.3247 | 22.138 |
| 57.0 | 110 | 0.2598 | 26.56241 |
| 63.4 | 013 | 0.2273 | 29.39718 |
| 66.3 | 020 | 0.3247 | 20.24587 |
| 68.5 | 112 | 0.2598 | 24.98152 |
| 69.1 | 021 | 0.3168 | 20.4182 |
| **AVERAGE CRYSTALLITE SIZE = 23.96** | | | |

The average crystallite size of *C. acuminata* extracts with $ZnCl_2$ and $Zn(CH_3COO)_2{\cdot}2H_2O$ as precursors ZnO was found to be 17.12 nm and 14.69 nm whereas *C. nitidia* extracts with $ZnCl_2$ and $Zn(CH_3COO)_2{\cdot}2H_2O$ as precursors was

B

| 2θ | hkl | FWHM (β) | D (nm) |
|---|---|---|---|
| 31.8 | 010 | 0.3572 | 21.14267 |
| 34.7 | 002 | 0.5845 | 12.82474 |
| 36.4 | 011 | 0.6494 | 11.4881 |
| 47.8 | 012 | 0.4546 | 15.79597 |
| 56.8 | 110 | 0.6494 | 10.63688 |
| 62.9 | 013 | 0.2598 | 25.77846 |
| 68.0 | 112 | 1.2672 | 5.136291 |
| **AVERAGE CRYSTALLITE SIZE = 14.69** | | | |

***Table 2.*** *Average crystallite size calculation for C. nitidia extracts with $ZnCl_2$ (C) and $Zn(CH_3COO)_2{\cdot}2H_2O$ (D) as precursors.*

C

| 2θ | hkl | FWHM (β) | D (nm) |
|---|---|---|---|
| 31.8 | 010 | 0.3572 | 21.14513 |
| 34.4 | 002 | 0.1948 | 38.50679 |
| 36.3 | 011 | 0.2922 | 25.54079 |
| 47.5 | 012 | 0.2273 | 31.62084 |
| 57.1 | 110 | 0.1948 | 35.41213 |
| 62.8 | 013 | 0.3572 | 18.7609 |
| 67.9 | 020 | 0.2922 | 22.28287 |
| 68.5 | 112 | 0.2598 | 24.99273 |
| 69.1 | 021 | 0.3168 | 20.42033 |
| **AVERAGE CRYSTALLITE SIZE = 23.68** | | | |

D

| 2θ | hkl | FWHM (β) | D (nm) |
|---|---|---|---|
| 31.7 | 010 | 0.3247 | 23.26381 |
| 34.4 | 002 | 0.2922 | 25.67309 |
| 36.3 | 011 | 0.3247 | 22.98305 |

also found to be 23.68 nm and 23.96 nm respectively.

*FTIR results*

FTIR was employed for the determination of the functional groups on the biosynthesized ZnO NPs in the range of 400-4000 $cm^{-1}$ as illustrated in Figure 4.

The presence of functional groups such as alcohols, phenols, amines, carboxylic acids from the organic extract from the FTIR results can interact with the zinc surface and aid in the stabilization of

particles. The spectra peaks observed between 440-458 $cm^{-1}$ corresponds to the Zn-O bond stretching vibrations for all the synthesized samples.

The broad absorption peaks observed between 3400–3600 $cm^{-1}$ in all the samples represent the stretching vibration mode of –OH groups. Though, the peaks are very strong in the case of ZnO NPs synthesized with $ZnCl_2$ (Fig 4 A&B), weak peaks were observed in ZnO NPs synthesized with $Zn(CH_3COO)_2{\cdot}2H_2O$ (Fig 4 C&D). This could be as a result of different concentration levels of phytochemical compounds present in the different plant species. Table 3 summarizes the different absorption peaks identified in the different samples as against previous studies with different plant extracts.

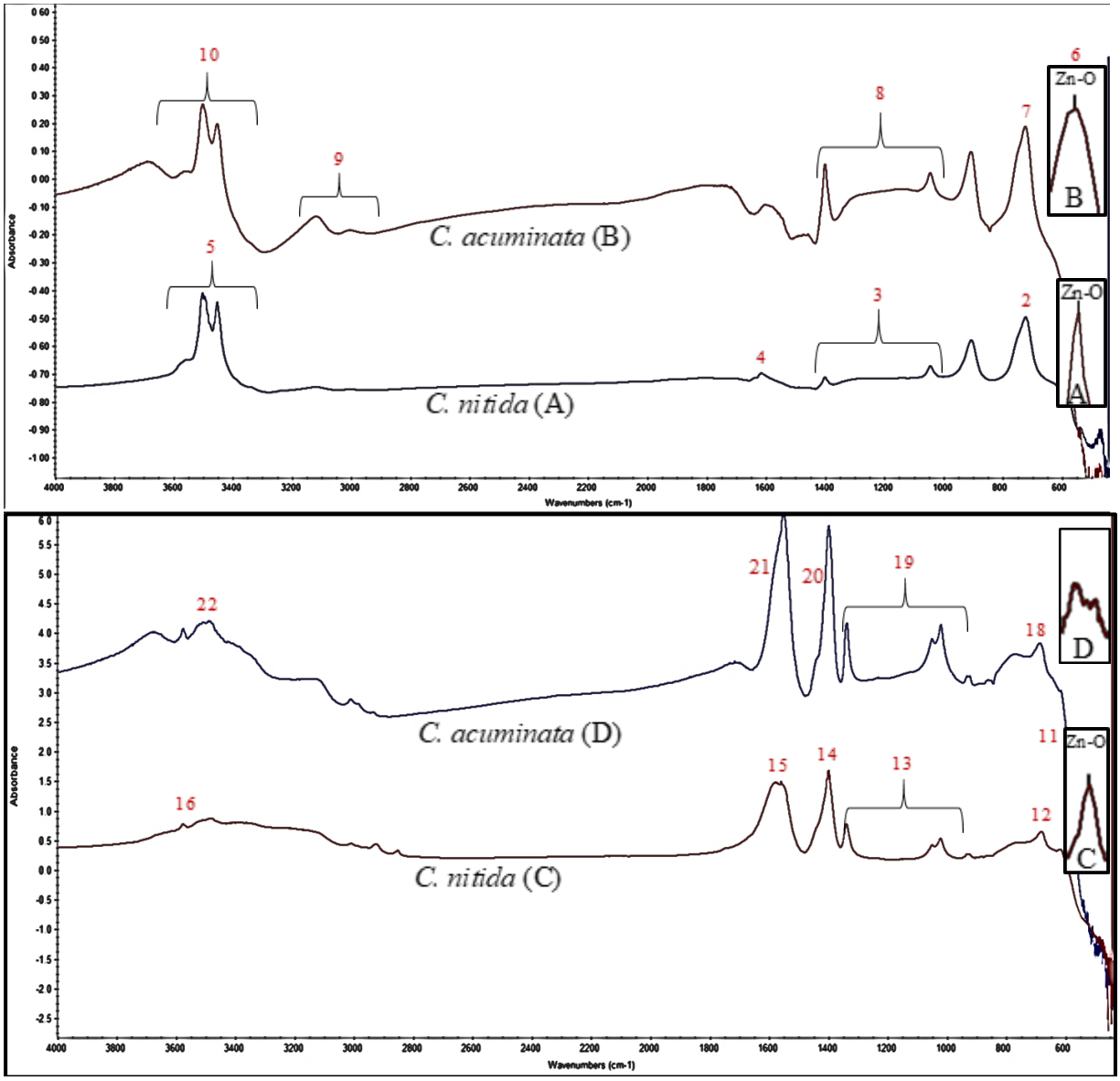


***Figure 4.*** *FT-IR spectra of ZnO NPs synthesized with $ZnCl_2$ from methanol extract of (A) C. nitida (B) C. acuminate, and FT-IR spectra of ZnO NPs synthesized with $Zn(CH_3COO)_2{\cdot}2H_2O$ from methanol extract of (C) C. nitida (D) C. acuminata*

***Table 3.*** *FT-IR spectral peaks of synthesized ZnO NPs from methanol extracts of leaves of C. nitida and C. acuminata using $ZnCl_2$ and $Zn(CH_3COO)_2 \cdot 2H_2O$ as precursor.*

| Plant | Zn – O | C – Cl | C – N | C = C | C = O | N – H | = C – H | C – C | O – H | Ref. |
|---|---|---|---|---|---|---|---|---|---|---|
| ***C. acuminate,*** **$ZnCl_2$** | 440.90 (6) | 722.54 (7) | 1043.72-1399.47 (8) (amine) | - | - | 3000-3117.49 (9) (amide) | - | - | 3451.36-3504.82 (10) | Current study |
| ***C. nitida,*** **$ZnCl_2$** | 445.16 (1) | 723.01 (2) | 1044.35-1398.88 (3) (amine) | - | 1748.60 (4) (aldehyde /ester) | - | - | - | 3451.88-3690.10 (5) | |
| ***C. acuminata*** **Zn(Ac)** | 458.27 (17) | - | 1049.78-1338.75 (19) (amine) | 1575.95 (20) | 1619 (21) | - | 680.35 (18) (alkene) | - | 3562.18 (22) | |
| ***C. nitida*** **Zn(Ac)** | 451.23 (11) | - | 1019.93-1397.54 (13) (amine) | 1551.41 (14) | 1614.69 (15) | - | 686.98 (12) (alkene) | - | 3490.27 (16) | |
| ***C. papaya*** **Leaf** | 441.74 | - | 1022.65-1336.44 | 1629.16 | 1629.16 | 1548..65 | - | - | 3474.38 | [33] |
| ***C. papaya*** **Stem-bark** | 444.08 | 683.59 | 1019.60-1338.44 | 1629.05 | 1629.05 | 1548.69 | - | - | 3474.61 | [33] |
| ***Laurus nobilis L.*** **Leaves** | 1634 & 600, 450 | - | - | - | - | - | - | - | 3300 | [48] |
| ***Corymbia citriodora*** **Leaf** | - | - | 1053 (amine) | 1520 | - | 1620 | - | 1431 | 3300 | [51] |
| ***Vaccinium arctostaphylos L.*** **Fruit** | 530 | - | - | - | 1638 | - | - | - | 3100-3648 | [28] |
| ***Trifolium pretense*** **Flower** | 515 | - | - | 2168 | 1383 | - | - | - | 2345, 1599 | [35] |

| | | | | | | | | | | |
|---|---|---|---|---|---|---|---|---|---|---|
| ***Passiflora caerulea* Leaf** | 532.35 | 650.01 | 1018.99, 1213.23 | 1429.25-1541.12 | 1429.25-1541.12 | 3304.06 (amide) | - | - | 3321.42 | [29] |
| ***Albizia lebbeck* Stem-bark** | 618 | - | - | - | 1030 (amide) | - | 1402 | - | 3356 | [31] |
| ***Asadhatoda (adulsa)*** or **Lemongrass** | - | - | - | 1645 | 1701 (ester) 1725 (amide) | 3115-3245 | - | - | - | [54] |
| ***Thespesia populnea* Leaf** | - | - | - | - | 1623 | - | - | - | 3412 | [55] |

*UV-Vis Analysis*

Figure 5 displays the UV–Visible absorption spectrum of synthesized ZnO NPs from methanol extracts of *C. nitida* and *C. acuminata* using $ZnCl_2$ and $(ZnCH_3COO)_2{\cdot}2H_2O$ as precursor in the range of 300-400 nm. The distinct absorption peak of the UV-vis analysis for ZnO NPs synthesized using $ZnCl_2$ as precursor for both *C. nitida* and *C. acuminata* (Fig 5 A & B) are observed at 365.30 and 370.80 nm respectively [28,56]. Though, Fig 5B gave a second peak at 344.80 nm, which may be due to quantum confinement effect [57], the two samples demonstrated the presence of ZnO with particles smaller than the bulk (380 nm).

ZnO NPs synthesized with $Zn(CH_3COO)_2{\cdot}2H_2O$ from methanol extract of *C. nitida* and *C. acuminata* (Fig 5 C&D) showed an intensive absorption at 368.90 and 364.70 nm respectively which is in conformity with the results in some studies [31]. In addition, [12], also reported the UV–vis absorption peak for ZnO NPs using *Pseudomonas aeruginosa* and zinc nitrate as precursor with particle size between 35-80 nm at 360 nm. Fig 5D also showed a shift in absorption peak to 340 nm due to quantum size effect as indicated in Fig 5B.

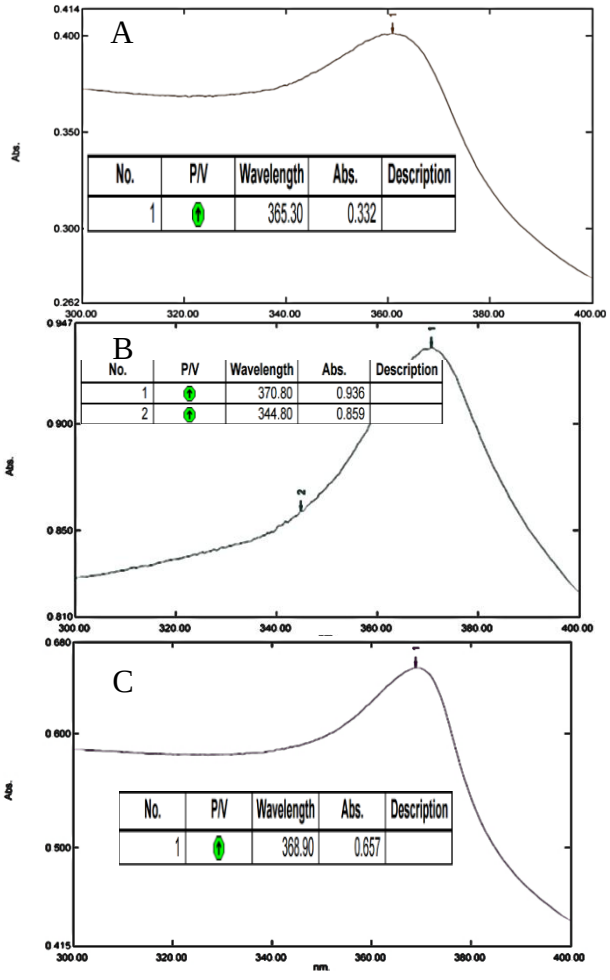

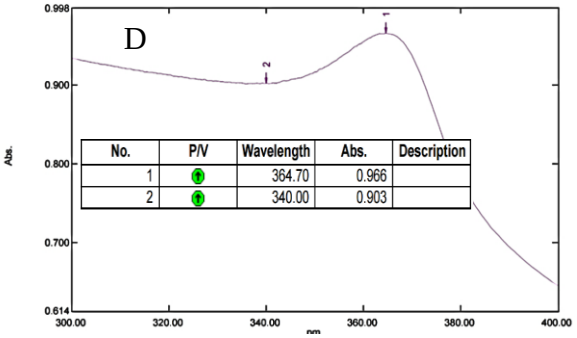


***Figure 5.*** *UV-Visible spectra of ZnO NPs synthesized with $ZnCl_2$ from methanol extract of (A) C. nitida (B) C. acuminate, and UV-Visible spectra of ZnO NPs synthesized with $Zn(CH_3COO)_2{\cdot}2H_2O$ from methanol extract of (A) C. nitida (B) C. acuminate.*

In totality, the results of our study showed the absorption peak for the synthesized ZnO NPs to be in conformity with the range of light absorption of ZnO NPs, which is 360–380 nm [58].

*EDX and AAS Analysis*

The elemental composition of the synthesized ZnO NPs as illustrated by the EDX plot (Fig 6 A-D) revealed the presence of Zn, O and C as the main constituents in the samples. Although some traces of Chlorine could be identified in (Fig 6 A & B) which may be due to effect of the constituents of the $ZnCl_2$ precursor. From the analysed samples, the average component of Zn, O and C present was 69.5%, 14.8% and 11.1% respectively as illustrated in Table 4. This result is in conformity with the study by [28]. The

***Table 4.*** *Elemental composition of synthesized ZnO NPs of samples*

| Sample type | % Zn | % O | % C |
|---|---|---|---|
| A | 66.16 | 16.28 | 12.35 |
| B | 68.07 | 13. 43 | 11.80 |
| C | 71.57 | 14.81 | 11.15 |
| D | 72.27 | 14.85 | 9.07 |

AAS detected elemental Zinc at 213.9 nm wavelength indicating the presence of the ZnO in the synthesized NPs. The calculated average percentage weight of Zn in the analysed samples using AAS technique was 71.37%.

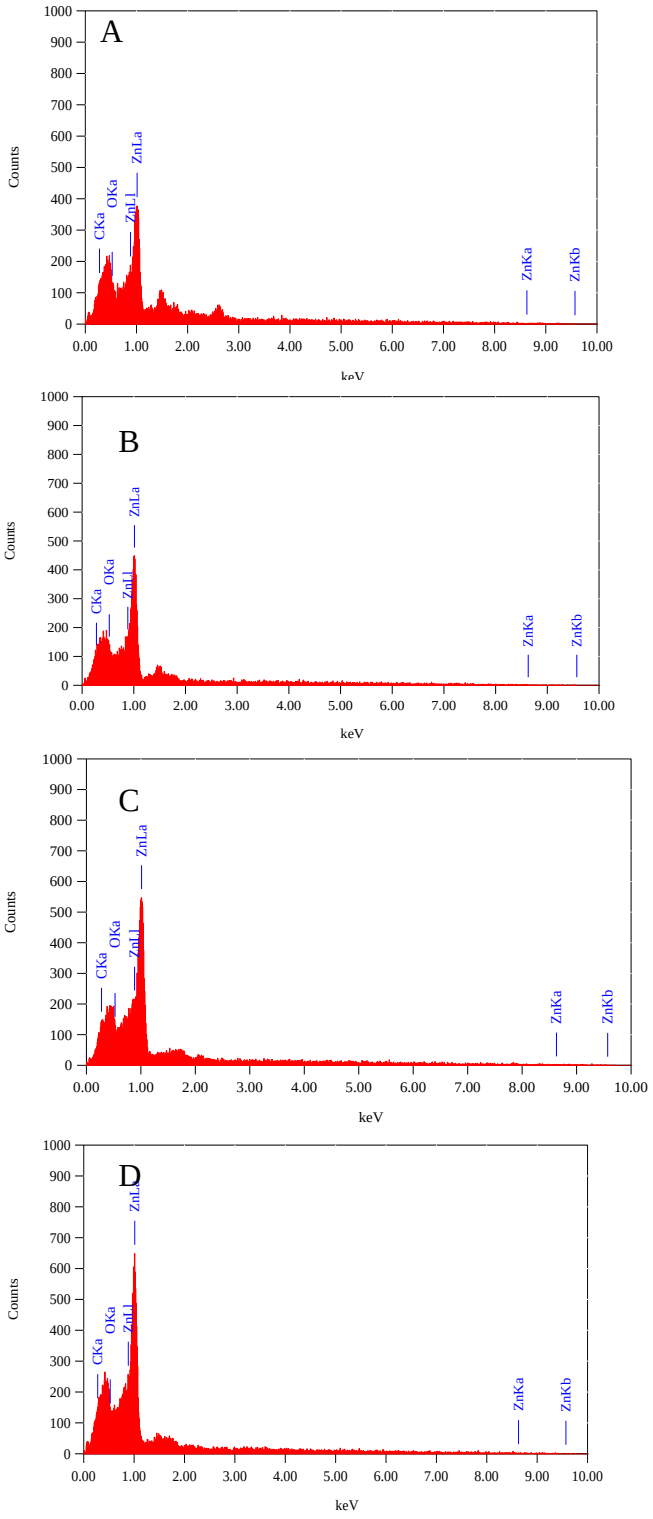


***Figure 6.*** *EDX analyses of ZnO NPs synthesized with $ZnCl_2$ from methanol extract of (A) C. nitida Leaf (B) C. acuminata Leaf and with*

*$Zn(CH_3COO)_2{\cdot}2H_2O$ from methanol extract of (C) C. nitida Leaf (D) C. acuminata Leaf*

*Antibacterial Efficacy*

The zone of inhibition against the selected microbes as a result of the activity of the ZnO NPs is illustrated in Tables 5 and 6.

***Table 5.*** *Effect of zinc oxide (ZnO) nanoparticle synthesized from methanol extract of Fresh leaves of C. acuminata and C. nitida on S. aureus, (Gram +ve), E. coli (Gram–ve), A. baumanni (Gram –ve), E. aquaticum (Gram +ve) and K. Pneumonia (Gram -ve): Precursor- $ZnCl_2$*

| | | Extract | | | | |
|---|---|---|---|---|---|---|
| Conc. (ppm) | Plant Part | *E. coli* (Gram –ve), | *S. aureus, (Gram +ve)* | *A. baumanni* (Gram –ve) | *E. aquaticum (*Gram +ve) | *K. pneumonia* (Gram -ve) |
| | Control | 2.04 ± 0.13<br>2.04 ± 0.09 | 2.03 ± 0.12<br>2.06 ± 0.22 | 2.09 ± 0.17<br>2.02 ± 0.02 | 2.08 ± 0.11<br>2.09 ± 0.13 | 2.11 ± 0.14<br>2.11 ± 0.10 |
| 25 | *C. acuminata* | 0.34 ± 0.13 | 0.45 ± 0.14 | 0.40 ± 0.15 | 0.45 ± 0.19 | 0.38 ± 0.14[b] |
| | *C. nitida* | 0.43 ± 0.31[b] | 0.35 ± 0.13 | 0.50 ± 0.13 | 0.53 ± 0.18 | 0.33 ± 0.11[b] |
| 50 | *C. acuminata* | 0.38 ± 0.23 | 0.51 ± 0.21 | 0.49 ± 0.24 | 0.52 ± 0.16 | 0.45 ± 0.18[b] |
| | *C. nitida* | 0.46 ± 0.10 | 0.42 ± 0.18 | 0.53 ± 0.22 | 0.57 ± 0.15[b] | 0.51 ± 0.17 |
| 100 | *C. acuminata* | 0.49 ± 0.21 | 0.52 ± 0.14 | 0.50 ± 0.16 | 0.58 ± 0.16 | 0.53 ± 0.13[b] |
| | *Cola nitida* | 0.51 ± 0.12 | 0.47 ± 0.14 | 0.60 ± 0.13 | 0.60 ± 0.06 | 0.55 ± 0.34[b] |
| 250 | *C. acuminata* | 0.53 ± 0.13 | 0.61 ± 0.13 | 0.56 ± 0.18 | 0.60 ± 0.17 | 0.58 ± 0.15[b] |
| | *C. nitida* | 0.53 ± 0.14 | 0.53 ± 0.12 | 0.66 ± 0.18 | 0.67 ± 0.17 | 0.61 ± 0.18[b] |
| 500 | *C. acuminata* | 0.56 ± 0.10 | 0.65 ± 0.11[b] | 0.60 ±0.19 | 0.63 ± 0.24 | 0.63 ± 0.17[b] |
| | *C. nitida* | 0.56 ± 0.10 | 0.57 ± 0.13 | 0.83 ± 0.17[b] | 0.73 ± 0.12 | 0.67 ± 0.19 |
| 1000 | *C. acuminata* | 0.63 ± 0.12[a] | 1.10 ± 0.10[a] | 1.84 ± 0.12 | 0.74 ± 0.13[a] | 0.70 ± 0.16[b] |
| | *C. nitida* | 0.98 ± 0.06[ab] | 0.67 ± 0.10[a] | 0.90 ± 0.11[a] | 0.74 ± 0.09[a] | 0.79 ± 0.16[a] |

***Table 6.*** *Effect of zinc oxide (ZnO) nanoparticle synthesized from methanol extract of Fresh leaves of C. acuminata and C. nitida on S. aureus, (Gram +ve), E. coli (Gram–ve), A. baumanni (Gram –ve), E. aquaticum (Gram +ve) and K. Pneumonia (Gram -ve): Precursor- $Zn(CH_3COO)_2{\cdot}2H_2O$*

| | | Extract | | | | |
|---|---|---|---|---|---|---|
| Conc. (ppm) | Plant Part | *E. coli* (Gram –ve), | *S. aureus, (Gram +ve)* | *A. baumanni* (Gram –ve) | *E. aquaticum (*Gram +ve) | *K. Pneumonia* (Gram -ve) |
| | Control | 2.05 ± 0.17<br>2.07 ± 0.14 | 2.03 ± 0.13<br>2.11 ± 0.11 | 2.04 ± 0.11<br>2.04 ± 0.10 | 2.05 ± 0.13<br>2.08 ± 0.03 | 2.09 ± 0.11<br>2.13 ± 0.13 |
| 25 | *C. acuminata* | 0.43 ± 0.31 | 0.35 ± 0.18 | 0.50 ± 0.13 | 0.52 ± 0.16[b] | 0.50 ± 0.11 |
| | *C. nitida* | 0.40 ± 0.08[b] | 0.35 ± 0.15 | 0.64 ± 0.11 | 0.46 ± 0.13 | 0.52 ± 0.14 |
| 50 | *C. acuminata* | 0.47 ± 0.22 | 0.49 ± 0.10[b] | 0.55 ± 0.22 | 0.58 ± 0.16[b] | 0.54 ± 0.14 |
| | *C. nitida* | 0.42 ± 0.09 | 0.36 ± 0.10[b] | 0.70 ± 0.26 | 0.50 ± 0.07[b] | 0.55 ± 0.11 |
| 100 | *C. acuminata* | 0.49 ± 0.19 | 0.50 ± 0.18 | 0.60 ± 0.11 | 0.68 ± 0.12 | 0.56 ± 0.07 |
| | *C. nitida* | 0.44 ± 0.19 | 0.40 ± 0.14 | 0.74 ± 0.14 | 0.68 ± 0.09 | 0.64 ± 0.13 |
| 250 | *C. acuminata* | 0.53 ± 0.17 | 0.62 ± 0.25 | 0.66 ± 0.16 | 0.71 ± 0.13 | 0.59 ± 0.18 |
| | *C. nitida* | 0.58 ± 0.13 | 0.48 ± 0.17 | 0.76 ± 0.12 | 0.77 ± 0.19[b] | 0.77 ± 0.16 |
| 500 | *C. acuminata* | 0.96 ± 0.16 | 0.66 ± 0.17 | 0.69 ±0.17 | 0.77 ± 0.19 | 0.61 ± 0.08[b] |
| | *C. nitida* | 0.66 ± 0.14 | 0.51 ± 0.14 | 0.85 ± 0.11 | 0.83 ± 0.13 | 0.88 ± 0.09[b] |
| 1000 | *C. acuminata* | 1.00 ± 0.13[a] | 0.73 ± 0.31[a] | 1.00 ± 0.19[a] | 0.94 ± 0.19[a] | 0.83 ± 0.13[a] |
| | *C. nitida* | 0.78 ± 0.12[a] | 0.68 ± 0.13[a] | 1.00 ± 0.08[ab] | 0.99 ± 0.10[a] | 0.93 ± 0.06[a] |

Research for biosynthesized ZnO NPs for reliable antibacterial drugs accelerated during the past two decades because of the increased occurrence in resistant of bacterial strains against antibiotic. On the other hand, characteristics exhibited by nanoparticles such as small size, surface area, surface reactivity, charge, and shape necessitated for the fabricating these biosynthesized drugs. There is no research conducted on the effect of zinc oxide (ZnO) nanoparticle synthesized from methanol extract of Fresh leaves of *C. acuminata* and *C. nitida* on *S. aureus*, (Gram +ve), *E. coli* (Gram –ve), *A. baumanni* (Gram –ve), *E. aquaticum* (Gram +ve) and *K. Pneumonia* (Gram -ve) using $ZnCl_2$ and $Zn(CH_3COO)_2{\cdot}2H_2O$ as precursors.

In the current research, inhibition of microbes from ZnO NPs from both extracts using the two precursors increased with increasing concentration (50-1000 ppm). From Table 5, whiles *A baumanni* recorded the highest inhibition of approximately 88% for *C. acuminata* in the 1000 ppm concentration of the ZnO NPs, *C. nitidia* recorded 45% using $ZnCl_2$ as precursor. Conversely, *E. coli* recorded the least inhibition of approximately 16-30% from extract of *C. acuminata* with increasing concentration. ZnO NPs from *C. acuminata* extract gave an inhibition of 22-54% in *S. aureus* (Gram +ve) than *E. aquaticum* (Gram +ve) of 21-35% as concentration increases from 25-1000 ppm. In the case of negative microbes used in this research, *A. baumanni* recorded the highest rate of inhibition when both extracts of the ZnO NPs were used. The variation in morphological compositions between the Gram –ve and Gram +ve bacteria may be the factor for the variations in microbes (antibacterial) sensitivity. Moreover, concentration and nature of the ZnO NPs has tremendous impact on the activity of microbes resulting in the damaging of the membrane and cytoplasmic contents [59]. It may be that the antioxidant contents in the *C. nitida* are higher than *C. acuminata* or the extract of *C. nitida* was properly biosynthesized as compared to *C. acuminata.*

From Table 6, ZnO NPs synthesized from methanol extract of Fresh leaves of *C. acuminata* and *C. nitida* against *A. baumanni* (Gram –ve) using $Zn(CH_3COO)_2{\cdot}2H_2O$ as precursor exhibited the highest effect of approximately 49% as compared to the other microbes used at concentration of 1000 ppm. Generally, inhibition rate increased with increasing concentration of the ZnO NPs from 25-1000 ppm. *S. aureus* recorded the least inhibition of 17-35% and 16-32% for the two ZnO NPs extracts.

Low inhibition of antibacterial activity may not necessary mean that there are no bioactive compounds in the plant species or the biosynthesized extracts has no biological activities against bacteria. Age, climatic and environmental factors of the plant samples, condition of synthesized ZnO NPs or small amounts of active compositions in the biosynthesized extract to show the antibacterial activity could be the reason. It was observed that, both plant species have potential active constituents for biological activities against the named bacteria in both precursors of $ZnCl_2$ and $Zn(CH_3COO)_2{\cdot}2H_2O$.

## 4. CONCLUSIONS

In conclusion, successful synthesis of the biosynthesized ZnO NPs from the two species of Cola (*C. nitida* and *C. acuminata*) leaves, confirmed the presence of ZnO in the samples through FT-IR, AAS, XRD, UV-vis and EDX techniques. Morphologically, SEM micrograph recorded spherical and flake-like nanostructures for *C. nitida* and *C. acuminate* respectively. *C. nitida* seems to record a greater particle size compared to *C. acuminata* for both precursors used in the study. As per the TEM analysis, *C. acuminata* recorded average particle size

of 43.26 nm and 32.15 nm for $ZnCl_2$ and $Zn(CH_3COO)_2{\cdot}2H_2O$ respectively whereas *C. nitida* recorded 69.12 nm and 84.26 nm for the average particle sizes for $ZnCl_2$ and $Zn(CH_3COO)_2{\cdot}2H_2O$ respectively. On the other hand, crystallite size from XRD analysis was in the range of 14.69-84.26 nm. Data provided from Table 5 and 6 showed that, ZnO NPs from *C. acuminata* using the two precursors, $ZnCl_2$ and $Zn(CH_3COO)_2{\cdot}2H_2O$ gave the highest inhibition of 88% and 49% respectively in the microbe, *A. aureus.*

The results proved that the methanol extract of both *C. nitida* and *C. acuminata* Leaf sampled from the central part of Ghana which was biologically synthesized with ZnO NPs using two precursors ($ZnCl_2$ and $Zn(CH_3COO)_2{\cdot}2H_2O$) showed potential antibacterial activity.

## ACKNOWLEDGMENT

The authors acknowledge the contribution of colleagues from Faculty of Resource Science and Technology (FRST) Geochemistry Laboratory and Analytical Laboratory, Universiti Malaysia Sarawak. This research was supported by Universiti Malaysia Sarawak, Tun Openg Chair, with Research Grant Code: F07/TOC/1738/ 2018.

## REFERENCES

1. Jones, K. E., Patel, N. G., Levy, M. A., Storeygard, A., Balk, D., Gittleman, J. L., Daszak, P., (2008). "Global trends in emerging infectious diseases", *Nature,* 451 (7181): 990–993.
2. Khan, S. T., Musarrat, J., Al-Khedhairy, A. A., (2016). "Countering drug resistance, infectious diseases, and sepsis using metal and metal oxides nanoparticles, current status", *Colloids Surf B Biointerfaces,* 146: 70–83.
3. Kumar, R.., Umar, A., Kumar, G., Nalwa, H. S., (2017). "Antimicrobial properties of ZnO nanomaterials: a review", *Ceram Int.,* 43: 3940–3961.
4. Yah, C. S., Simate, G. S., (2015). "Nanoparticles as potential new generation broad spectrum antibacterial agents", *DARU Journal of Pharmaceutical Sciences,* 23(1): 43.
5. Vimbela, G. V., Ngo, S. M., Fraze, C., Yang, L., Stout, D. A., (2017). "Antibacterial properties and toxicity from metallic nanomaterials", *International journal of nanomedicines,* 12: 3941.
6. Nowack, B., Bucheli, T. D., (2007). "Occurrence, behavior and effects of nanoparticles in the environment", *Environmental pollution,* 150(1): 522.
7. Bhattacharya, R., Mukherjee, P., (2008). "Biological properties of naked metal nanoparticles", *Advanced Drug Delivery Reviews,* 60(11): 1289-1306.
8. Sharma, V. K., Yngard, R. A., Lin, Y., (2009). "Silver nanoparticles: green synthesis and their antibacterial activities", *Advances in colloid and interface science,* 145(1-2): 83-96.
9. Shah, M., Fawcett, D., Sharma, S., Tripathy, S. K., Poinern, G. E. J., (2015). "Green synthesis of metallic nanoparticles via biological entities", *Materials,* 8(11): 7278-7308.
10. Stankic, S., Suman, S., Haque, F., Vidic, J., (2016). "Pure and multi metal oxide nanoparticles: synthesis, antibacterial and cytotoxic properties", *J. Nanobiotechnol.,* 14(1): 73.
11. Nel, A., Xia, T., Mädler, L., Li, N., (2006). "Toxic potential of materials at the nanolevel", *Science,* 311(5761): 622-627.
12. Singh, B. N., Rawat, A. K. S., Khan, W., Naqvi, A. H., Singh, B. R., (2014). "Biosynthesis of stable antioxidant ZnO nanoparticles by *Pseudomonas aeruginosa* rhamnolipids", *PLoS One,* 9 (9): 106937.
13. Peralta-Videa, J. R., Huang, P. Y., Parsons, J., Zhao, L., Lopez-Moreno, L., Hernandez-Viezcas, J. A., Gardea-Torresdey, J. L., (2016). "Plant-based green synthesis of metallic nanoparticles: scientific curiosity or a realistic alternative to chemical synthesis?", *Nanotechnol Environ Eng.,* 1(1): 4.
14. Hu, S-H., Chen, Y-C., Hwang, C-C., Peng, C-H., Gong, D-C., (2010). "Development of a wet chemical method for the synthesis of arrayed ZnO nanorods", *J. Alloy. Comp.,* 500 (2): L17–L21.
15. Wang, A., Ng, H. P., Xu, Y., Li, Y., Zheng, Y., Yu, J., Han, F., Peng, F., Fu, L., (2014). "Gold nanoparticles: synthesis, stability test, and application for the rice growth", *J. Nanomater.,* Article ID 451232.
16. Chen, Y., Zhang, C., Huang, W., Situ, Y., Huang, H., (2015). "Multimorphologies nano-ZnO preparing through a simple solvothermal method for photocatalytic application", *Mater. Lett.,* 141: 294–297.
17. Tien, H. N., Khoa, N., Hahn, S. H., Chung, J. S., Shin, E. W., Hur, S. H., (2013). **"**One-pot synthesis of a reduced graphene oxide – zinc oxide sphere composite and its uses as a visible light photocatalyst", *Chem. Eng. J.,* 229: 126–133.

18. Khorsand, Z. A., Wang, H. Z., Yousefi, R., Moradi, G. A., Ren, Z. F., (2013). "Sonochemical synthesis of hierarchical ZnO nanostructures", *Ultrason. Sonochem.,* 20 (1): 395–400.
19. Omri, K., Najeh, I., Dhahri, R., El Ghoul, J., El mir, L., (2014). "Effects of temperature on the optical and electrical properties of ZnO nanoparticles synthesized by sol-gel method", *Microelectron. Eng.,* 128: 53–58.
20. Khorsand, Z. A., Abrishami, M. E., Abd Majidi, W. H., Yosefi, R., Hosseini, S. M., (2011). "Effects of annealing temperature on some structural and optical properties of ZnO nanoparticles prepared by a modified sol-gel combustion method", *Ceram. Inter.,* 37(1): 393–398.
21. Wang, Y., Zhang, C., Bi, S., Luo, G., (2010). "Preparation of ZnO nanoparticles using the direct precipitation method in a membrane dispersion micro-structured reactor", *Powder Technol.,* 202(1-3): 130–136.
22. Sundrarajan, M., Ambika, S., Bharathi, K., (2015). "Plant-extract mediated synthesis of ZnO nanoparticles using *Pongamia pinnata* and their activity against pathogenic bacteria", *Adv. Powder Technol.,* 26: 1294-99.
23. Olad, A., Ghazjahaniyan, F., Nosrati, R., (2018). "A Facile and Green Synthesis Route for the Production of Silver Nanoparticles in Large Scale", *Int. J. Nanosci. Nanotechnol.,* 14(4): 289-296.
24. Geoprincy, G., Vidhya srri, B. N., Poonguzhali, U., Nagendra, N. G., Renganathan, S., (2014). "A review on green synthesis of silver nanoparticles", *Asian J. Pharm. Clin. Res*., 6(1): 8–12.
25. Ahmed, S., Ahmad, M., Swami, B. L., Ikram, S., (2016). "A review on plants extract mediated synthesis of silver nanoparticles for antimicrobial applications: a green expertise", *J. Adv Res.,* **7**(1): 17–28.
26. Soltanabad, M. H., Bagherieh-Najjar, M. B., Baghkheirati, E. K., Mianabadi, M., (2018). "Ag-Conjugated Nanoparticle Biosynthesis Mediated by Rosemary Leaf Extracts Correlates with Plant Antioxidant Activity and Protein Content", *Int. J. Nanosci. Nanotechnol*., 14(4): 319-325
27. Ghanbari, M., Bazarganipour, M., Salavati-Niasari, M., (2017). "Photodegradation and removal of organic dyes using cui nanostructures, green synthesis and characterization", *Separation and Purification Technology*, 173: 27-36,
28. Mohammadi-Aloucheh, R., Habibi-Yangjeh, A., Bayrami, A., Latifi-Navid, S., Asadi, A., (2018). "Enhanced anti-bacterial activities of ZnO nanoparticles and ZnO/CuO nanocomposites synthesized using *Vaccinium arctostaphylos L.* fruit extract", *Artificial Cells, Nanomedicine, and Biotechnology*, 46(1): 1200-1209.
29. Santhoshkumar, J., Kumar, V. S., Rajeshkumar, S., (2017). "Synthesis of zinc oxide nanoparticles using plant leaf extract against urinary tract infection pathogen", *Resource-Efficient Technologies*, 3, 459–465.
30. Fatimah, I., Aftrid, Z. H. V. I., (2019). "Characteristics and antibacterial activity of green synthesized silver nanoparticles using red spinach (*Amaranthus tricolor L.*) leaf extract", *Green Chem. Lett. and Revs.,* 12(1): 25–30.
31. Umar, H., Kavaz, D., Rizaner, N., (2019). "Biosynthesis of zinc oxide nanoparticles using *Albizia lebbeck* stem bark, and evaluation of its antimicrobial, antioxidant, and cytotoxic activities on human breast cancer cell lines", *Int. J. Nanomed.,* 14: 87–100
32. Rotimi, L, Ojemaye, M. O., Okoh, O. O., Sadimenko, A., Okoh, A. I., (2019). Synthesis, characterization, antimalarial, antitrypanocidal and antimicrobial properties of gold nanoparticle, *Green Chem. Lett and Revs.,* 12(1): 61–68
33. Droepenu, E. K., Asare, E. A., (2019). "Morphology of green synthesized ZnO nanoparticles using low temperature hydrothermal technique from aqueous *Carica papaya* extract", *Nanoscience and Nanotechnology*, 9(1): 29-36.
34. Divya, M. J., Sowmia, C., Joona, K., Dhanya, K. P., (2013). **"**Synthesis of zinc oxide nanoparticles from *Hibiscus rosa-sinensis* leaf extract and investigation of its antimicrobial activity", *Res. J. Pharm. Biol. Chem.,* 4(2): 1137-1142.
35. Dobrucka, R., Dugaszewska, J., (2015). "Biosynthesis and antibacterial activity of ZnO nanoparticles using *Trifolium pratense* flower extract", *Saudi J. of Biological Sci.,* 23(4): 517-523.
36. Shah, R. K., Boruah, F., Parween, N., (2015). "Synthesis and Characterization of ZnO Nanoparticles using Leaf Extract of *Camellia sinesis* and Evaluation of their Antimicrobial Efficacy", *Int. J. Curr. Microbiol. App. Sci.,* 4(8): 444-450
37. Sundaramurthy, N., Parthiban, C., (2015). "Biosynthesis of copper oxide nanoparticles using *Pyrus pyrifolia* leaf extract and evolve the catalytic activity", *Int. Res. J. of Eng. and Technol. (IRJET),* 2(6), 332-338.
38. Reddy, L. S., Nisha, M. M., Joice, M., Shilpa, P. N., (2014). "Antibacterial activity of zinc oxide (ZnO) nanoparticle against Klebsiella pneumonia", *Pharmaceutical biology,* 52(11): 1388-1397.
39. http://en.wikipedia.org/wiki/kolanut
40. Jayeola, C. O., (2001). "Preliminary studies on the use of kolanuts (Cola nitida) for soft drink production", *J. Food Technol. Afr*., 6(1): 25-26.
41. Attfield, J., (1865). "On the food value of the kolanut – a new source of theine", *Pharm. J.,* 6: 457.
42. Blades, M., (2000). "Functional foods or neutraceutical", *Nutr. Food Sci.,* 30(2): 73-75.

43. Naczk, M., Shahidi, F., (2006). “Phenolics in cereals, fruits and vegetables: Occurrence, extraction and analysis”, *J. Pharm. Biomed. Anal.*, 41: 1523–1542.
44. Umaru, I. J., Fasihuddin, B. A., Otitoju, O. O., Hauwa, A. U., (2018). “Phytochemical Evaluation and Antioxidant Properties of Three Medicinal Plants Extracts”, *Med. & Anal. Chem. Int. J. Phytochem. Eval.*, 2(2): 1-8.
45. Yang, K., Lin, D., Xing, B., (2009). “Interactions of humic acid with nanosized inorganic oxides”, *Langmuir*, 25(6): 3571–3576.
46. Umaru, I. J., Fasihuddin, A. B., Zaini, B. A, Umaru, H. A., (2018b). “Antibacterial and cytotoxic actions of chloroform crude extract of Leptadenia hastata(pers)Decnee”, *Clinical Medical Biochem.*, 4: 1-4.
47. Shadrokh, Z., Yazdani, A., Eshghi, H., (2017). “Study on Structural and Optical Properties of Wurtzite Cu2ZnSnS4 Nanocrystals Synthesized via Solvothermal Method”, *Int. J. Nanosci. Nanotechnol.*, 13(4): 359-366.
48. Divya, M. J., Sowmia, C., Joona, K., Dhanya, K. P., (2013). “Synthesis of zinc oxide nanoparticle from Hibiscus rosa-sinensis leaf extract and investigation of its antimicrobial activity”, *Res. J. Pharm. Biol. Chem. Sci.*, 4(2): 1137–1142.
49. Fakhari, S., Jamzad, M., Fard, H. K., (2019). “Green synthesis of zinc oxide nanoparticles: a comparison”, *Green Chem. Lett and Revs*., 12(1): 19–24
50. Geetha, A., Sakthivel, R., Mallika, J., Kannusamy, R., Rajendran, R., “Green synthesis of antibacterial zinc oxide nanoparticles using biopolymer Azadirachta indica Gum”, *Orient. J. Chem.*, 2016; 32: 955-963.
51. Zheng, Y., Fu, L., Han, F., Wang, A., Cai, W., Yu, J., Yang, J., Peng, F., (2015). “Green biosynthesis and characterization of zinc oxide nanoparticles using *Corymbia citriodora* leaf extract and their photocatalytic activity”, *Green Chem. Lett. and Revs.*, 8(2): 59–63.
52. Daphedar, A., Taranath, T. C., (2018). “Green synthesis of zinc nanoparticles using leaf extract of Albizia saman (Jacq.) Merr. and their effect on root meristems of Drimia indica (Roxb.) Jessop”, *Caryologia*., 71: 93-102.
53. Khatami, M., Alijani, H. Q., Heli, H., Sharifi, I., (2018). “Rectangular shaped zinc oxide nanoparticles: Green synthesis by Stevia and its biomedical efficiency”, *Ceram. Int.*, 44: 15596-602.
54. Anvekar, T. S., Chari, V. R., Kadam, H., (2017). “Green Synthesis of ZnO Nano Particles, its Characterization and Application”, *Mater. Sci. Res. India*, 14(2): 153-157.
55. Gowsalya, V., Santhiya, E., Chandramohan, K., (2017). “Synthesis, characterization of ZnO nanoparticles from *Thespesia populnea”, Indian J. Appl. Res.*, **7**(10): 542-543.
56. Shankar S, Rhim J W., (2017). “Facile approach for large-scale production of metal and metal oxide nanoparticles and preparation of antibacterial cotton pads”, *Carbohydr Polym.*, 163: 137–145.
57. Soosen, S. M., Lekshmi, B., George, K. C., (2009). “Optical properties of ZnO nanoparticles”, *Academic Rev.*, 57-65.
58. Nagarajan, S., Arumugam, K. K., (2013). “Extracellular synthesis of zinc oxide nanoparticle using seaweeds of gulf of Mannar”, *India. J. Nanobiotechnol.*, 11: 39.
59. Divyapriya, S., Sowmia, C., Sasikala, S., (2014). **“**Synthesis of zinc oxide nanoparticles and antimicrobial activity of Murraya koenigi”, *World J. Pharm Sci.*, 3(12): 1635-1645.